Journal of Zhejiang University-SCIENCE A (Applied Physics & Engineering)
ISSN 1673-565X (Print); ISSN 1862-1775 (Online)
www.zju.edu.cn/jzus; www.springerlink.com
E-mail: jzus@zju.edu.cn

Effect of weld reinforcement on axial plastic buckling of welded steel cylindrical shells*

Chu-lin YU, Zhi-ping CHEN†‡, Ji WANG, Shun-juan YAN, Li-cai YANG

(*Institute of Process Equipment, Zhejiang University, Hangzhou 310027, China*)

†E-mail: zhiping@zju.edu.cn

Received July 21, 2011; Revision accepted Dec. 14, 2011; Crosschecked Dec. 29, 2011

Abstract: The effect of weld reinforcement on axial plastic buckling of welded steel cylindrical shells is investigated through experimental and numerical buckling analysis using six welded steel cylindrical shell specimens. The relationship between the amplitude of weld reinforcement and the axial plastic buckling critical load is explored. The effect of the material yield strength and the number of circumferential welds on the axial plastic buckling is studied. Results show that circumferential weld reinforcement represents a severe imperfect form of axially compressed welded steel cylindrical shells and the axial plastic buckling critical load decreases with the increment of the mean amplitude of circumferential weld reinforcement. The material yield strength and the number of circumferential welds are found to have no significant effect on buckling waveforms; however, the axial plastic buckling critical load can be decreased to some extent with the increase of the number of circumferential welds.

Key words: Cylindrical shells, Axial buckling, Plastic, Weld, Reinforcement, Geometric imperfections
doi:10.1631/jzus.A1100196 **Document code:** A **CLC number:** O39

1 Introduction

Axially compressed welded steel cylindrical shells have a wide application in engineering (Chen *et al*., 2009). Axial elastic or plastic buckling is the key point in their design (Simitses, 1986). Many researchers have investigated the effect of different initial geometric imperfections on elastic or plastic buckling of cylindrical shells (Teng, 1996; Mandal and Calladine, 2000; Donnel and Wan, 1950; Koiter, 1963; Hutchinson *et al*., 1971; Amazigo and Budiansky, 1972; Arbocz and Williams, 1977; Gellin, 1979; Yamaki, 1984; Elishakoff *et al*., 1985; Rotter and Teng, 1989; Krishnakumar and Foster, 1991; Holst *et al.*, 1999; Lancaster *et al.*, 2000; Teng and Song, 2001; Jamal *et al.*, 2003). It was found that the extent to which the buckling critical load is decreased depends on the shape and the amplitude of the initial geometric imperfections, and the worst initial geometric imperfection to a newly built cylindrical shell structure depends on the manufacturing process. Welded steel cylindrical shells in engineering are usually constructed by many curved steel panels. Circumferential welds rather than longitudinal welds between these curved panels are regarded as one of the worst initial geometric imperfections to axial elastic or plastic buckling of welded steel cylindrical shells (Rotter and Teng, 1989; Pircher and Bridge, 2001; Teng and Lin, 2005; Hübner *et al.*, 2006).

Clarke and Rotter (1988), Ding and Rotter (1992), Berry *et al.* (2000), Hornung and Saal (2002), Teng and Lin (2005) carried out experiments on the

‡ Corresponding author

* Project supported by the National High-Tech R&D (863) Program of China (No. 2009AA044803), the National Key Technologies R&D Program of China (No. 2011BAK06B02), and the Specialized Research Fund for the Doctoral Program of Higher Education (No. 20090101110051), China

shape of circumferential welds of thin welded cylindrical shells. White and Dwight (1977), Rotter and Teng (1989), Fritschi (2001), Steinhardt (2001), and Pircher (2001) proposed various shape functions for circumferential weld. Although these functions are not the same, they are all expressed as an inward radial depression. Circumferential welds deform inward when cylindrical shells are thin and proper precaution is not considered during welding. It is worth noting that the deformation of circumferential weld is not shaped as an inward radial depression if welded steel cylindrical shells have relatively thick wall and good counter-deformation measures are considered. Reasonable weld reinforcement should be used for heat-retaining and slow cooling which prevents the occurrence of coarse grain and large welding residual stress. Furthermore, weld reinforcement on the inner surface should be polished smoothly for other requirements. A cylindrical shell with one circumferential weld is shown in Fig. 1. Fig. 1c shows the shape of circumferential weld reinforcement; Figs. 1a and 1b show two classic axisymmetric depression shapes of circumferential weld proposed by Rotter and Teng (1989) that are named Type A and Type B respectively in this study.

It can be seen from Fig. 1c that the shape of circumferential weld reinforcement is a type of outward radial deformation, and it is quite different from Type A and Type B representing two types of inward radial deformation. Thus, the effect of circumferential weld reinforcement on the axial plastic buckling of cylindrical shells is quite different from that of Type A and Type B. Therefore, in this paper, the effect of circumferential weld reinforcement on the axial plastic buckling of welded steel cylindrical shells is studied experimentally and numerically. Three groups of cylindrical shell specimens with the same ratio of radius to wall thickness but different materials and different number of circumferential welds are manufactured. Their initial geometric imperfections and experimental axial plastic buckling critical loads are obtained through a self-made buckling platform. Nonlinear plastic buckling analysis is carried out through finite element analysis. The distribution characteristics of circumferential weld reinforcement in the axial and circumferential directions are analyzed. The relationship between the amplitude of circumferential weld reinforcement and the axial plastic buckling critical load is explored. Furthermore, the effect of the material yield strength and the number of circumferential welds on the axial plastic buckling is also investigated.

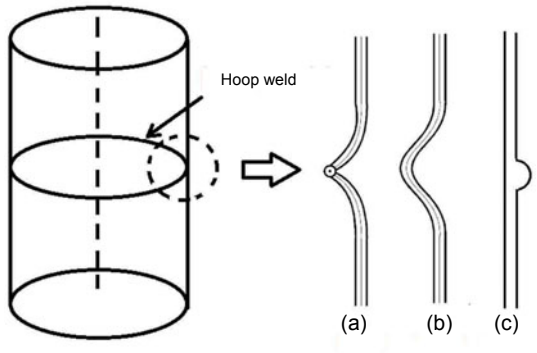

Fig. 1 Schematic diagram of three typical shapes of circumferential weld
(a) Type A; (b) Type B; (c) Circumferential weld reinforcement

2 Cylindrical shell specimens and experimental platform

2.1 Manufacture of the shell specimens

Since the initial geometric imperfections depend on the manufacturing process, it is necessary to choose the same manufacturing process of welded cylindrical shells. The experimental method is adopted to study the effect of the initial geometric imperfections on the axial plastic buckling behavior of welded cylindrical shells. There are two classic manufacturing methods of welded cylindrical shell specimens as found in the existing literature. The first manufacturing method was proposed by Schmidt and Swadlo (1996) where a single large flat plate was cut into several small flat plates followed by the welding of these small flat plates together to form a new large flat plate with patterned welds. Finally, this new large flat plate was rolled into a cylindrical shell specimen. The second manufacturing method was invented by Teng (2005) where two large flat plates were rolled into two semi-cylindrical shells followed by two longitudinal welding of the two semi-cylindrical shells to form a whole cylindrical shell specimen. However, the specimens made by Schmidt and Swadlo (1996) and Teng (2005) have one or two longitudinal welds through the height of the specimens, which are quite different from welded steel

cylindrical shells whose longitudinal welds are separated with each other. Typical manufacturing process of welded steel cylindrical shells is shown in Fig. 2.

Manufacturing process follows a sequence (Fig. 2) such that: cold rolling of flat plate→welding the first layer of cylindrical shell→welding the second layer of cylindrical shell at an offset degree with the first layer→up to the top layer of the cylindrical shell. The shell specimens used in this study are made step by step according to the above manufacturing process. In addition, both ends of the specimens are welded with rigid end rings with groove to avoid the pre-buckling deformation. To get relatively large amplitude of weld reinforcement, argon arc welding machine is used to weld the shell specimens under large thermal input and fast welding speed.

2.2 Design of the shell specimens

In order to study the effect of different material yield strength and different number of circumferential welds on plastic buckling, three groups of welded steel cylindrical shell specimens are made. Detail of the shell specimens is listed in Table 1. The specimens are given six digit identifiers such that R represents the inner radius, H represents the effective height of the specimens which is obtained by subtracting the height of the groove of the rigid end rings from the whole height of the shell specimens, the numbers after R and H represents the first two numbers of the inner radius and the effective height of the specimens. M1 and M2 represent the first material and second material. A and B represent two different patterns of welds such that A consists of two identical cylinders and has one circumferential weld and two longitudinal welds, B consists of three identical cylinders and has two circumferential welds and three longitudinal welds, and t represents the wall thickness. Here, take the specimen R40H39B for example, a plate of R40H39B after cold rolling is shown in Fig. 3a, the matching rigid end ring is shown in Fig. 3b, R40H39B assembled with two rigid end rings is shown in Fig. 3c, the rectangular box in Fig. 3c is shown in Fig. 3d. The other shell specimens assembled with rigid end rings except R40H39B are shown in Fig. 4.

Table 1 Description of the shell specimens

Specimen No.	Weld pattern	Material	t (mm)	R/t	H (mm)
R40H39A	A	M1	1.46	274.0	390.0
R40H39B	B				
R40H33A	A	M1	1.46	274.0	390.0
R40H33B	B				
R35H34A	A	M2	1.28	273.4	341.3
R35H34B	B				

2.3 Material mechanical properties

Three tensile specimens for each of material M1 and M2 are made. The initial portion of stress-strain curves are shown in Fig. 5. Typical experimental results of the elastic modulus E and the yield strength ReL are listed in Table 2.

Fig. 5 shows that the mechanical properties of M1 and M2 are different in terms of the magnitude

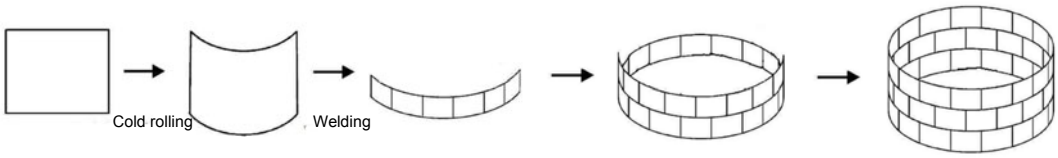

Fig. 2 Typical manufacturing process of welded steel cylindrical shells

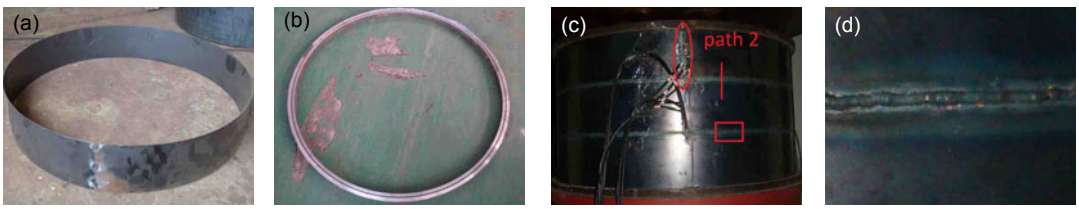

Fig. 3 Relative photos of the specimen R40H39B

(a) A plate after cold rolling; (b) Matching rigid end ring; (c) Specimen assembled with two rigid end rings; (d) Rectangular box shown in (c)

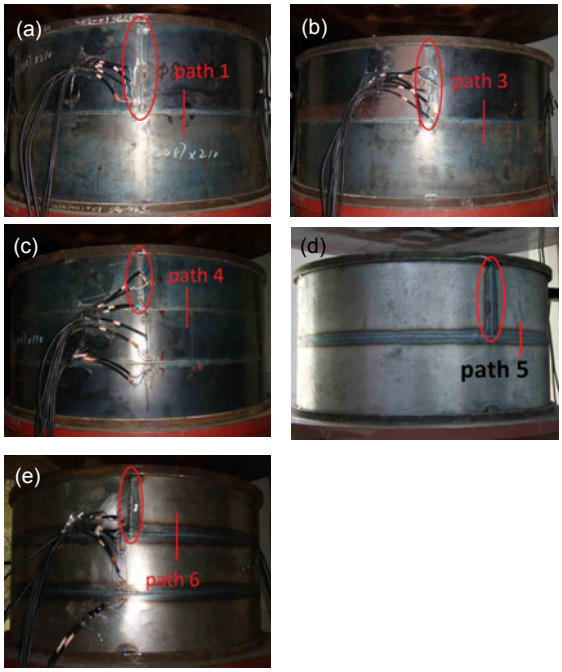

Fig. 4 Specimens assembled with rigid end rings
(a) R40H39A; (b) R40H33A; (c) R40H33B; (d) R35H34A; (e) R35H34B

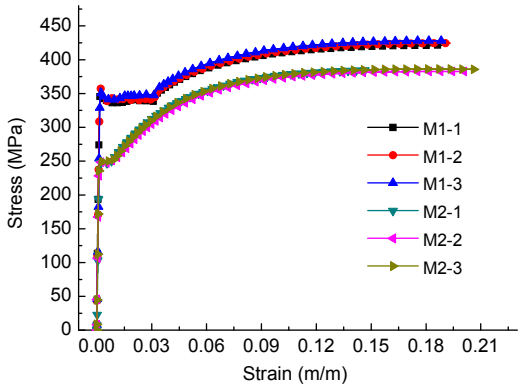

Fig. 5 Initial portion of stress-strain curves of the tensile specimens

Table 2 Typical results of the tensile specimens

Tensile specimen No.	*E* (MPa)	ReL (MPa)
M1-1	200779	335
M1-2	222449	340
M1-3	224808	340
M2-1	220961	250
M2-2	204875	250
M2-3	239350	255

of yield strength. Table 2 shows that the difference of the three tensile specimens of the same material is very small. In particular, the data of the tensile specimen M1-1 are a little lower than those of the other two (M1-2 and M1-3), and the data of the tensile specimen M2-2 are a little lower than those of the other two (M2-1 and M2-3). To be conservative, the mechanical properties of the tensile specimens M1-1 and M2-2 are used in numerical simulation.

2.4 Experimental platform set-up

In order to establish a quantitative relationship between the initial geometric imperfections and the experimental axial buckling critical load, and to construct a finite element (FE) model that incorporates the real initial geometric imperfections of the shell specimens, Arbocz and Williams (1977), Singer and Abramovich (1995), Berry *et al.* (2000), Pircher and Wheeler (2003), Teng and Lin (2005), and Stoffel (2006), etc., made different forms of equipment with automatic acquiring function of initial geometric imperfections of cylindrical shells. For the same purpose, an axial buckling experimental platform with automatic acquiring function of initial geometric imperfections and axial loading function by displacement control is also made. The photo of the experimental platform is shown in Fig. 6.

Fig. 6 Experimental platform

The principle of constructing the FE model of the shell specimen is as follows. The FE model consists of many quadrilateral elements where each element has four edges. Though these edges are straight, the details of the initial geometric imperfections of the shell specimens can be reflected precisely

as long as the imperfect surface of the shell specimens is meshed with enough elements. Furthermore, as elements consist of many nodes, these nodes can be seen as the test points of the shell specimen. If the real coordinates of these test points can be obtained, the real initial geometric imperfections of the shell specimens can be reflected by the FE model. Therefore, in this study, a high accuracy level (3 μm) laser displacement sensor (LK081, Keyence Company, Japan) is used to measure the radial coordinates of the test points. The laser displacement sensor is fixed on a screw which can change its motion from rotary to linear. The screw is fixed on a rotating frame which can rotate around the axis of the shell specimen. Thus, the laser displacement sensor can move along the axial direction of the shell specimen as well as can rotate around the axis of the shell specimen. The real coordinates of all test points can be determined. After the coordinates of the test points are got, Matlab software is used to assign the measured data to the nodes of the FE model.

To get the precise details of the initial geometric imperfections of the shell specimens and to satisfy the convergence requirement of FE analysis, enough test points should be set up in the circumferential and axial directions during the process of scanning initial geometric imperfection. Therefore, 254 and 109 test points are set up in the circumferential and axial direction respectively for the specimens with one circumferential weld, and 261 and 105 test points are set up in the circumferential and axial direction respectively for the specimens with two circumferential welds.

Although every effort is taken to make sure the precision of the measured geometric imperfections, it is worth noting that there still may be some misalignment error between the central axis of the shell specimen and the central axis of the rotating frame of the experimental platform. However, FEM results will not be affected significantly, as this error can be converted to a rigid displacement of the finite element model (Zhao, 2001).

3 Experimental results

In order to illustrate the initial distribution characteristics of circumferential weld reinforcement in the axial direction, a 100-mm long path across circumferential weld (located at 30° from the upper longitudinal weld (see the ellipse in Figs. 3c and 4 in counterclockwise direction) is adopted for every specimen. The schematic diagram of the six paths is shown in Figs. 3c and 4, and the two circumferential welds of the specimens with weld pattern B are given the name 1 and 2 respectively. The measured results are shown in Fig. 7. δ stands for the amplitude of circumferential weld reinforcement, Z represents the axial coordinate of test points on the path, and Z_w represents the axial coordinate of circumferential weld. Furthermore, for the purpose of illustrating the initial distribution characteristics of circumferential weld reinforcement in the circumferential direction, considering the specimen R40H39A for example, frequency histogram of the amplitude of circumferential weld reinforcement is shown in Fig. 8. The curve in Fig. 8 represents the probability density function of the normal distribution with mean value 1.033 and standard deviation 0.315. Experimental

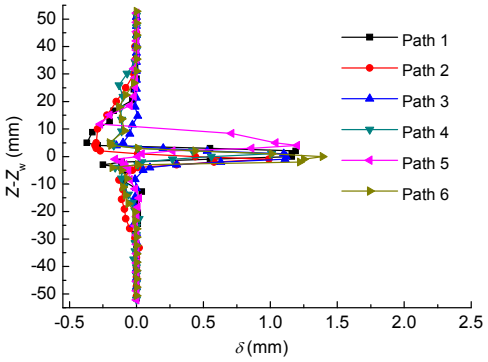

Fig. 7 Measured initial geometric imperfections of test points on paths 1–6

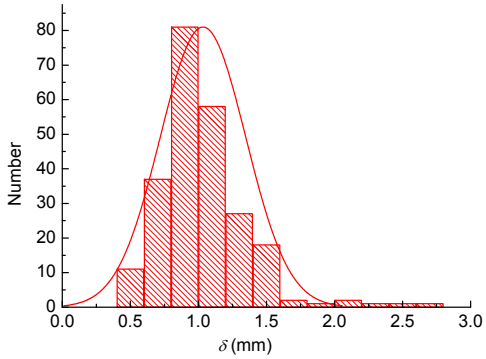

Fig. 8 Frequency histogram of the amplitude of circumferential weld reinforcement of the specimen R40H39A

buckling deformation of the specimens is shown in Fig. 9. The experimental relationship between axial load and axial displacement of all specimens is shown in Fig. 10.

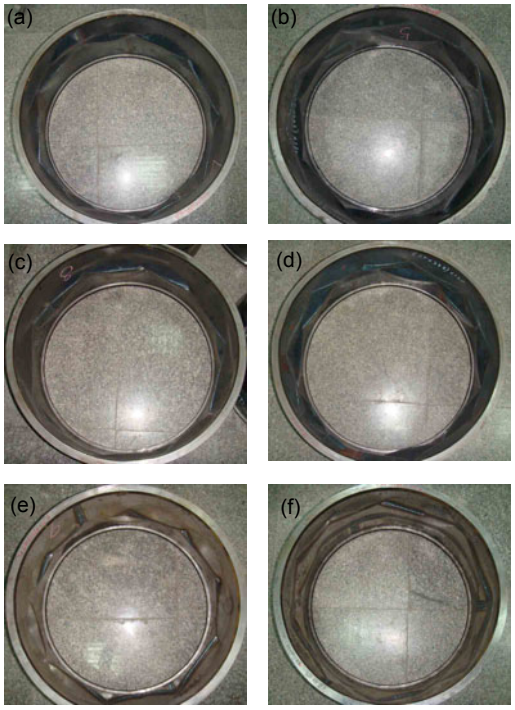

Fig. 9 Buckling deformation of the shell specimens
(a) R40H39A; (b) R40H39B; (c) R40H33A; (d) R40H33B; (e) R35H34A; (f) R35H34B

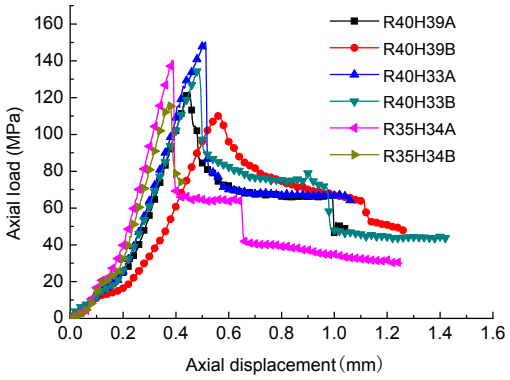

Fig. 10 Experimental relationship between axial load and axial displacement of all specimens

4 FEM procedures and results

4.1 FEM procedures

The large commercial FEM software ABAQUS is used for FE analysis. The element type S4R with seven integration points along the wall thickness direction is chosen. There are 27 432 and 27 144 elements for the specimens with weld patterns A and B respectively according to the test points set-up mentioned in Section 2.4. Both geometric and material nonlinearity are included. Material constitutive law is true stress-strain relationship based on the tensile test data. Mises yield criteria is used. The arc-length method is adopted to calculate the buckling critical load.

The buckling analysis is carried out assuming full clamping for both ends except that the top edge is allowed to have axial displacement. A rigid plate is defined to simulate the loading head of the experimental platform. Contact pairs are established to simulate the interaction between the pressure head and the upper edge of the cylindrical shell specimens. The axial load control in numerical simulation is displacement control, which means that the displacement is applied as load to the rigid plate directly. Then, the axial load can be obtained by the relationship of force and reaction force between the rigid plate and the shell specimen.

4.2 FEM results

Contours plots of buckling deformation of all specimens obtained by FE analysis are shown in Fig. 11 (magnified 10 times). Fig. 12 shows results of axial loads corresponding to axial displacement.

5 Results analysis and discussion

5.1 Distribution characteristics of circumferential weld reinforcement in the axial and circumferential directions

The initial distribution characteristics of the amplitude of circumferential weld reinforcement in the axial and circumferential directions are explored in this section. Fig. 7 shows that, there is an obvious outward bulge around the circumferential weld for all specimens in the axial direction. The maximum amplitude of circumferential reinforcement is about 1.47 mm. The width of circumferential weld reinforcement in the axial direction is very small such as 10 mm up and down from the centerline of circumferential weld. Moreover, the shape of circumferential weld reinforcement in the axial direction is almost

symmetrically distributed with respect to the centerline of circumferential weld. On the other hand, Fig. 8 shows that the distribution characteristics of circumferential weld reinforcement of R40H39A in the circumferential direction follow a normal distribution, which agrees well with the distribution characteristics of field measurements of circumferential weld depressions found in (Pircher *et al*., 2001).

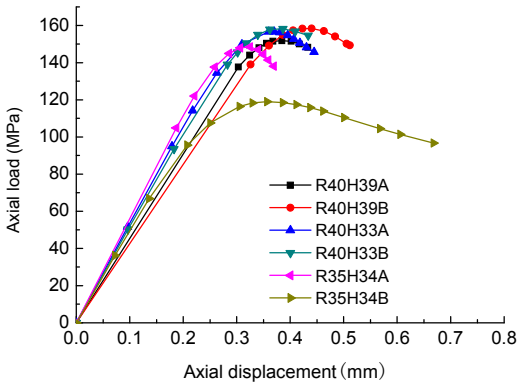

Fig. 12 Numerical results of axial load with respect to axial displacement of the specimens

5.2 Buckling deformation of welded cylindrical shells with weld reinforcement

The number of waveforms of circumferential weld at buckling obtained by experimental and FE analysis is listed in Table 3. n_{exp} and n_{FEM} represent the numbers of waveforms of circumferential weld obtained by experiment and FE analysis respectively, the symbol '/' is used to separate the number of waveforms of the specimens R40H39B, R40H33B and R35H34B with two circumferential welds, the

Table 3 Comparison of circumferential waveforms at buckling obtained by using experimental and numerical methods

Specimen No.	R/t	ReL (MPa)	n_{exp}	n_{FEM}
R40H39A	274.0	335	10	10
R40H39B			10/10	10/10
R40H33A	274.0	335	10	10
R40H33B			10/10	11/11
R35H34A	273.4	250	10	8
R35H34B			10/10	10/10

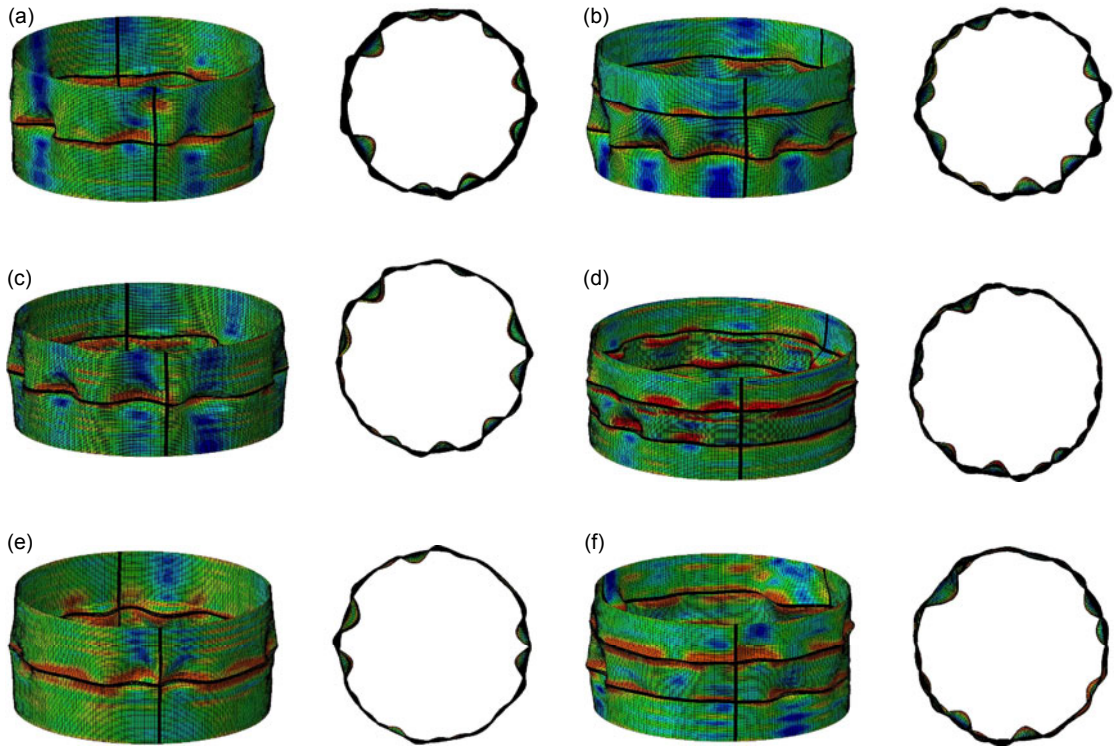

Fig. 11 Buckling deformation contours of the specimens obtained by FE analysis
(a) R40H39A; (b) R40H39B; (c) R40H33A; (d) R40H33B; (e) R35H34A; (f) R35H34B (magnified 10 times)

number before and after '/' represents the number of waveforms of the first and the second circumferential weld, respectively.

Figs. 9 and 11 show several concave waveforms around the circumferential weld for R40H39A, R40H33A and R35H34A. They also show many concave waveforms around the two circumferential welds where the waveforms of each circumferential weld separated from each other can be observed for R40H39B, R40H33B and R35H34B. The above results imply that circumferential weld reinforcement is the vital factor to the axial plastic buckling deformation. It is worth noting that the number of waveforms of circumferential weld obtained by experiment is the same for specimens of different yield strengths and different number of circumferential welds having similar ratio of radius to wall thickness. This illustrates that the number of waveforms of circumferential weld mainly depends on the ratio of radius to wall thickness rather than the material yield strength or the number of circumferential welds.

It can be seen from Table 3 that there is a good agreement between experimental and numerical results for all the specimens except R35H34A. Furthermore, Figs. 9 and 11 show that there is a difference between experimental and numerical buckling deformation in terms of the uniformity of waveforms in the circumferential direction. This phenomenon may be attributed to the neglecting of residual stress such as cold rolling and welding residual stress in numerical analysis.

5.3 Effect of the amplitude of circumferential weld reinforcement on the axial plastic buckling

It has been found in some previous researches that the effect of the amplitude on plastic buckling is much larger than the wavelength for an axisymmetric geometric imperfection defined by the amplitude and the wavelength (Hutchinson *et al.*, 1971; Rotter and Teng, 1989). Therefore, in this section, we will explore the effect of the amplitude of circumferential weld reinforcement on the axial plastic buckling critical load of welded steel cylindrical shells. It can be seen from Fig. 8 that the amplitude of circumferential weld reinforcement is randomly distributed in the circumferential direction. Thus, the mean amplitude of circumferential weld reinforcement $\overline{\delta}$ is used as the gauge to reflect the relationship between the amplitude of circumferential weld reinforcement and the axial plastic buckling critical load. Dimensionless ratio of the mean amplitude of circumferential weld reinforcement to wall thickness $\overline{\delta}/t$, dimensionless ratio of the axial plastic buckling critical load to the classical buckling load σ_{exp}/σ_{cl}, and dimensionless ratio of the experimental buckling critical load to the numerical buckling critical load $\sigma_{exp}/\sigma_{FEM}$ are listed in Table 4. In Table 4, for the specimens R40H39B, R40H33B, and R35H34B with two circumferential welds, data from the first and second rows represent $\overline{\delta}/t$ of the first and the second circumferential welds, respectively. The classical elastic buckling critical load is calculated as follows:

$$\sigma_{cl}=0.605Et/R. \tag{1}$$

Table 4 shows that the dimensionless mean amplitude of circumferential weld reinforcement $\overline{\delta}/t$ is in between 0.70 and 0.78 (the maximum value is adopted for the specimens with two circumferential welds), and the dimensionless experimental axial plastic buckling critical load σ_{exp}/σ_{cl} is in between 24.8% and 33.8% making circumferential weld reinforcement very severe compared to many other imperfection forms (Yamaki, 1984). This illustrates that the circumferential weld reinforcement is one of the worst initial geometric imperfections for welded steel cylindrical shells. Fig. 13

Table 4 Experimental and numerical results of the specimens

Specimen No.	R/t	ReL (MPa)	$\overline{\delta}/t$	σ_{exp}/σ_{cl} (%)	$\sigma_{exp}/\sigma_{FEM}$ (%)
R40H39A	274.0	335	0.71	27.8	75.8
R40H39B	274.0	335	0.75	24.8	78.7
			0.73		
R40H33A	274.0	335	0.70	33.8	96.2
R40H33B	274.0	335	0.72	30.4	85.5
			0.64		
R35H34A	273.4	250	0.72	30.9	94.3
R35H34B	273.4	250	0.78	25.8	98.0
			0.73		

shows the effect of the mean amplitude of circumferential weld reinforcement $\overline{\delta}/t$.

Fig. 13 shows that when the ratio of radius to wall thickness is fixed, although the material yield strength and the number of circumferential welds are different, the overall trend is that the axial plastic buckling critical load decreases with the increment of $\overline{\delta}/t$. Especially, as shown Fig. 13, although the material yield strength and the number of circumferential welds are different, $\overline{\delta}/t$ of R40H33B and R35H34A and the axial plastic buckling critical loads are almost the same. Moreover, $\overline{\delta}/t$ of R40H39A is smaller than those of R40H33B and R35H34A, while the axial plastic buckling critical loads of R40H33B and R35H34A are larger than that of R40H39A. Similarly, $\overline{\delta}/t$ of R40H39B is smaller than that of R35H34B, while the axial plastic buckling critical load of R35H34B is larger than that of R40H39B. The above phenomenon illustrate that, when the ratio of radius to wall thickness is fixed, the mean amplitude of circumferential weld reinforcement is the vital factor for the axial plastic buckling critical load. Nevertheless, the axial plastic buckling critical load depends not only on $\overline{\delta}/t$ but also on other factors such as the detail distribution of initial geometric imperfections, and so on. Implication of these findings is that, the amplitude of circumferential weld reinforcement should be reduced to raise the axial plastic buckling critical load of welded steel cylindrical shells.

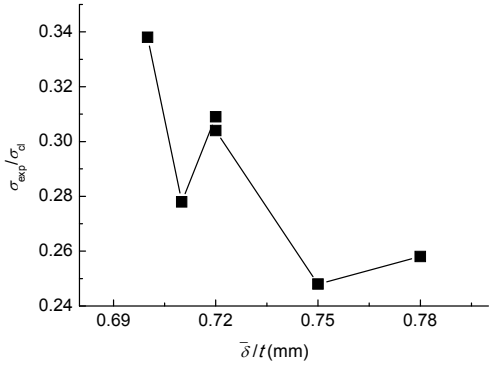

Fig. 13 Experimental axial buckling critical loads for dimensionless mean amplitude of circumferential weld

Table 4 shows that the values of $\sigma_{exp}/\sigma_{FEM}$ are smaller than 1, which implies that the numerical axial plastic buckling critical loads are a little higher than the experimental loads. This phenomenon may attribute to the fact that several factors, such as load eccentricity, residual stress (cold rolling and welding residual stress), etc. are not included in the numerical analysis.

It is worth noting that the shapes of the curves in Fig. 10 are different from those of the curves in Fig. 12. Especially, we can find that the slopes of the curves obtained by experiment are different from those of curves obtained by FE analysis at the initial loading and the post buckling stage. This is due to the fact that backlash in the bearing can cause nonlinear response at low loads in the initial loading and unloading. Though the testing frame is stiff, some components in load path (such as the universal joints) are not leading to an overall stiffness that is insufficient to capture the early part of the unloading curves (Berry *et al.*, 2000).

5.4 Effect of the number of circumferential welds on the axial plastic buckling critical load

Comparing the experimental axial buckling critical loads of R40H39A, R40H33A and R35H34A to those of R40H39B, R40H33B and R35H34B (the detail data are listed in Table 4), it can be realized that, the mean amplitude of circumferential weld reinforcement of the specimens with one circumferential weld is smaller than that of circumferential weld reinforcement of the specimens with two circumferential welds. This implies that welding deformation may increase with the increment of the number of circumferential welds. Moreover, the axial plastic buckling critical loads of the specimens with two circumferential welds are smaller than those of the specimens with one circumferential weld. The maximum difference is about 5.1%, which illustrates that the axial plastic buckling critical load will be decreased to some extent with the increase of the number of circumferential welds. It must be noted that the distance between the two circumferential welds may be much distant for the specimens with two circumferential welds. Therefore, the effect of the number of circumferential welds on axial plastic buckling should be checked further when one circumferential weld is close enough to the other.

It can be seen from Fig. 12 that the axial plastic

buckling load of R40H39A obtained by FE analysis is smaller than that of R40H39B, and numerical buckling load of R35H34A is larger than that of R35H34B. However, Fig. 10 shows that the experimental axial buckling plastic loads of the shell specimens with weld pattern A are larger than those of the shell specimens with weld pattern B. This phenomenon may be attributed to the fact that, several factors besides the initial geometric imperfections such as load eccentricity, residual stress (cold forming and welding residual stress), non-uniform material yield strength and wall thickness, etc., can affect the axial plastic buckling critical load. However, in results from FE analysis, these factors are not included. Moreover, although much effort is taken to assure the accuracy of acquired FE model, some error may still existed between actual physical model and FE model for which the experimental and numerical axial plastic buckling loads may have a difference.

6 Conclusions

The effect of weld reinforcement on axial plastic buckling of welded steel cylindrical shells is investigated through experiment and FE analysis in this study. Six shell specimens with the same ratio of radius to wall thickness but of different material yield strength and different number of circumferential welds are produced by the same manufacturing process of welded steel cylindrical shells in engineering. Some conclusions can be drawn:

1. The initial axial shape of circumferential weld reinforcement of the shell specimens is almost symmetrically distributed with respect to the centerline of circumferential weld. The amplitude of circumferential weld reinforcement decreases rapidly in the axial direction, while its distribution characteristic in the circumferential direction follows a normal distribution.

2. Circumferential weld reinforcement represents a severe imperfect form for axially compressed welded steel cylindrical shells. For laboratory shell specimens, the axial plastic buckling deformation of these specimens is characterized by many concave waveforms around the circumferential weld. The mean amplitude of circumferential weld reinforcement is about 0.70–0.78 times of wall thickness and the experimental buckling critical loads are in the range of 24.8%–33.8% of classical elastic buckling critical load. The mean amplitude of circumferential weld reinforcement is a decisive factor to the axial plastic buckling critical load, which implies that it is important to control the mean amplitude of circumferential weld reinforcement in order to raise the axial buckling critical load.

3. The experimental buckling waveforms of circumferential weld are the same for the six shell specimens with the same ratio of radius to thickness but different material yield strength. This indicates that the material yield strength does not have a significant effect on the buckling waveforms of circumferential weld for welded steel cylindrical shells with weld reinforcement.

4. The number of circumferential welds has a large effect on buckling deformation, while it has little effect on the number of buckling waveforms of circumferential weld. Furthermore, the axial plastic buckling critical load could be decreased to some extent with the increase of the number of circumferential welds.

5. FE analysis of the nonlinear plastic buckling gives good predictions of experimental results for most shell specimens. However, for some specimens, there are still some discrepancies between the experimental and the numerical results in terms of the uniformity of waveforms of circumferential weld at buckling and the axial plastic buckling critical load. This phenomenon may be attributed to the facts that load eccentricity, residual stress (cold rolling and welding residual stress), non-uniform material yield strength and wall thickness are not included in numerical analysis.

References

Amazigo, J.C., Budiansky, B., 1972. Asymptotic formulas for the buckling stresses of axially compressed cylinders with localized or random axisymmetric imperfections. *Journal of Applied Mechanics*, **39**(1):179-184. [doi:10.1115/1.3422608]

Arbocz, J., Williams, J.G., 1977. Imperfection surveys on a 10-ft-diameter shell structure. *AIAA Journal*, **15**(7):949-956. [doi:10.2514/3.7389]

Berry, P.A., Rotter, J.M., Bridge, R.Q., 2000. Compression

tests on cylinders with circumferential weld depressions. *Journal of Engineering Mechanics*, **126**(4):405-413. [doi:10.1061/(ASCE)0733-9399(2000)126:4(405)]

Chen, Z.P., Sun, B., Yu, C.L., Zeng, M., 2009. Finite-element analysis of liquid-storage tank foundations using settlement difference as boundary condition. *Proceedings of the Institution of Mechanical Engineers Part E: Journal of Process Mechanical Engineering*, **221**(3):119-127. [doi:10.1243/09544089JPME256]

Clarke, M.J., Rotter, J.M., 1988. A Technique for the Measurement of Imperfections in Prototype Silos and Tanks. Technical Report No. R565, University of Sydney, Australia.

Ding, X.L., Rotter, J.M., 1992. The Measurement of Imperfections in Full-Scale Steel Silos. International Conference on Bulk Materials Handling and Transportation, Wollongong, Australia, p.467-472.

Donnel, L.H., Wan, C.C., 1950. Effect of imperfections on buckling of thin cylinders and columns under axial compression. *Journal of Applied Mechanics*, **17**(1):73-83.

Elishakoff, I., Vanmanen, S., Vermeulen, P.G., Arbocz, J., 1985. First-order second-moment analysis of the buckling of shells with random initial imperfections. *AIAA Journal*, **25**(8):1113-1117. [doi:10.2514/3.9751]

Gellin, S., 1979. Effect of axisymmetric imperfection on the plastic buckling of an axially compressed cylindrical shell. *Journal of Applied Mechanics*, **46**(1):125-131. [doi:10.1115/1.3424483]

Holst, J.M.F.G., Rotter, J.M., Calladine, C.R., 1999. Imperfections in cylindrical shells resulting from fabrication misfits. *Journal of Engineering Mechanics*, **125**(4):410-418. [doi:10.1061/(ASCE)0733-9399(1999)125:4(410)]

Hornung, U., Saal, H., 2002. Buckling loads of tank shells with imperfections. *International Journal of Non-Linear Mechanics*, **37**(4-5):605-621. [doi:10.1016/S0020-7462(01)00087-7]

Hübner, A., Teng, J.G., Saal, H., 2006. Buckling behavior of large steel cylinders with patterned welds. *International Journal of Pressure Vessels and Piping*, **83**(1):13-26. [doi:10.1016/j.ijpvp.2005.10.003]

Hutchinson, J.W., Tennyson, R.C., Muggeridge, D.B., 1971. Effect of a local axisymmetric imperfection on the buckling behavior of a circular cylindrical shell under axial compression. *AIAA Journal*, **9**(1):48-52. [doi:10.2514/3.6123]

Jamal, M., Lahlou, L., Midani, M., Zahrouni, H., Limam, A., Damil, N., Potier-Ferry, M., 2003. A semi-analytical buckling analysis of imperfect cylindrical shells under axial compression. *International Journal of Solids and Structures*, **40**(5):1311-1327. [doi:10.1016/S0020-7683(02)00583-8]

Koiter, W.T., 1963. The Effect of Axisymmetric Imperfections on the Buckling of Cylindrical Shells under Axial Compression. Proc. Koninklijke Nederlandse Akademie van Wetenschappen, the Netherland, p.265-279 (in Dutch).

Krishnakumar, S., Foster, C.G., 1991. Axial load capacity of cylindrical shells with local geometric defects. *Experimental Mechanics*, **31**(2):104-110. [doi:10.1007/BF02327560]

Lancaster, E.R., Calladine, C.R., Palmer, S.C., 2000. Paradoxical buckling behaviour of a thin cylindrical shell under axial compression. *International Journal of Mechanical Sciences*, **42**(5):843-865. [doi:10.1016/S0020-7403(99)00030-2]

Mandal, P., Calladine, C.R., 2000. Buckling of thin cylindrical shells under axial compression. *International Journal of Solids and Structures*, **37**(33):4509-4525. [doi:10.1016/S0020-7683(99)00160-2]

Pircher, M., Bridge, R.Q., 2001. The influence of circumferential weld-induced imperfections on the buckling of silos and tanks. *Journal of Constructional Steel Research*, **57**(5):569-580. [doi:10.1016/S0143-974X(00)00027-4]

Pircher, M., Wheeler, A., 2003. The measurement of imperfections in cylindrical thin-walled members. *Thin-Walled Structures*, **41**(5):419-433. [doi:10.1016/S0263-8231(02)00096-4]

Pircher, M., Berry, P.A., Ding, X., Bridge, R.Q., 2001. The shape of circumferential weld-induced imperfections in thin-walled steel silos and tanks. *Thin-Walled Structures*, **39**(12):999-1014. [doi:10.1016/S0263-8231(01)00047-7]

Rotter, J.M., Teng, J.G., 1989. Elastic stability of cylindrical shells with weld depressions. *Journal of Structural Engineering*, **115**(5):1244-1263. [doi:10.1061/(ASCE)0733-9445(1989)115:5(1244)]

Schmidt, H., Swadlo, P., 1996. Two Buckling Tests Demonstrating the Influence of the Pattern of Geometrical and Structural Imperfections on the Axial Compressive Buckling Strength of Cylindrical Shells. Proceedings, International Workshop on Imperfections in Metal Silos, INSA, Lyon, France, p.181-190.

Simitses, G.J., 1986. Buckling and postbuckling of imperfect cylindrical shells: a review. *Applied Mechanics Reviews*, **39**(10):1517-1524.

Singer, J., Abramovich, H., 1995. The development of shell imperfection measurement techniques. *Thin-Walled Structures*, **23**(1-4):379-398. [doi:10.1016/0263-8231(95)94361-V]

Stoffel, M., 2006. An experimental method for measuring the buckling shapes of thin-walled structures. *Thin-Walled Structures*, **44**(1):69-73. [doi:10.1016/j.tws.2005.08.012]

Teng, J.G., 1996. Buckling of thin shells: Recent advances and trends. *Applied Mechanics Reviews*, **49**(4):263-274. [doi:10.1243/09544089JPME256]

Teng, J.G., Song, C.Y., 2001. Numerical models for nonlinear analysis of elastic shells with eigenmode-affine imperfections. *International Journal of Solids and Structures*, **38**(18):3263-3280. [doi:10.1016/S0020-7683(00)00222-5]

Teng, J.G., Lin, X., 2005. Fabrication of small models of large cylinders with extensive welding for buckling experiments. *Thin-Walled Structures*, **43**(7):1091-1114.

[doi:10.1016/j.tws.2004.11.006]
White, J.D., Dwight, J.B., 1977. Weld Shrinkage in Large Stiffened Tubulars. Proceedings of a Conference on Residual Stresses in Welded Constructions, the Welding Institute, London, UK, p.337-348.
Yamaki, N., 1984. Elastic Stability of Circular Cylindrical Shells. Elsevier, Amsterdam, North-Holland, p.20-35.
Zhao, Y., 2001. Stability and Strength of Steel Silo Transition Junctions. PhD Thesis, the Hong Kong Polytechnic University, Hong Kong.